

# Learning Spatially Decoupled Color Representations for Facial Image Colorization

Hangyan Zhu<sup>1</sup>, Ming Liu<sup>1,\*</sup>, Chao Zhou<sup>2</sup>, Zifei Yan<sup>1</sup>, Kuanquan Wang<sup>1</sup>, Wangmeng Zuo<sup>1</sup>

<sup>1</sup>Harbin Institute of Technology, Harbin, China, <sup>2</sup>Shanghai Transsion Co, Ltd., Shanghai, China  
cshyzhu@outlook.com, csmliu@oulook.com, wzmzuo@hit.edu.cn

## Abstract

Image colorization methods have shown prominent performance on natural images. However, since humans are more sensitive to faces, existing methods are insufficient to meet the demands when applied to facial images, typically showing unnatural and uneven colorization results. In this paper, we investigate the facial image colorization task and find that the problems with facial images can be attributed to an insufficient understanding of facial components. As a remedy, by introducing facial component priors, we present a novel facial image colorization framework dubbed FCNet. Specifically, we learn a decoupled color representation for each face component (*e.g.*, lips, skin, eyes, and hair) under the guidance of face parsing maps. A chromatic and spatial augmentation strategy is presented to facilitate the learning procedure, which requires only grayscale and color facial image pairs. After training, the presented FCNet can be naturally applied to facial image colorization with single or multiple reference images. To expand the application paradigms to scenarios with no reference images, we further train two alternative modules, which predict the color representations from the grayscale input or a random seed, respectively. Extensive experiments show that our method can perform favorably against existing methods in various application scenarios (*i.e.*, no-, single-, and multi-reference facial image colorization). The source code and pre-trained models will be publicly available.

## Introduction

Image colorization aims at predicting the color for grayscale images, which can be utilized for a variety of tasks such as old photo restoration, advertising, and art creation (Iizuka and Simo-Serra 2019; Qu, Wong, and Heng 2006; Tsafaris et al. 2014; Vitoria, Raad, and Ballester 2020). With years of development, a series of image colorization methods (Zhang, Isola, and Efros 2016; Deshpande et al. 2017; Wu et al. 2021; Kang et al. 2023; Weng et al. 2024) have been presented, and user assistance, as well as reference images, are also introduced for user-intended colorization results (Levin, Lischinski, and Weiss 2004; Chia et al. 2011; Huang, Zhao, and Liao 2022; Wang et al. 2023). These methods have achieved prominent image colorization performance on natural images.

Among various image contents, faces are a category of special objects that should be carefully considered. On the

one hand, faces are very common in images, especially in old photos where faces are the main subject of photography in the early years, which poses a great demand for facial image colorization. On the other hand, faces are one of the most familiar objects for us. Thus, humans are sensitive to faces and can perceive subtle anomalies in facial images, making facial image colorization quite challenging. In our experiments, when applying existing image colorization methods to faces, they tend to produce unnatural and uneven results, which are insufficient to meet the user requirements.

The failure of existing methods on facial images motivates us to develop a face-oriented image colorization method. In this paper, we investigate the facial image colorization task and find that the problem of existing methods on facial images mainly lies in an insufficient understanding of facial components. For example, sometimes the generated colors of the upper and lower parts of the cheek are significantly different, which can be attributed to the image colorization models not realizing that the cheek is a whole component and the color is usually consistent. To remedy such a phenomenon and generate visually pleasing results, we propose a novel facial image colorization framework dubbed FCNet by introducing facial component priors.

Specifically, we force the model to possess the knowledge of face structures and learn a decoupled color representation for each facial component. To begin with, a pre-trained face parsing model is introduced, which provides the segmentation of facial components as a prior. The explicitly introduced facial component prior greatly alleviates the burden of the colorization modules. Then, an encoder can be deployed to learn the color representations. However, even with the face component priors, the color representations of different face components are still entangled, which may cause the problem of color infiltration (*i.e.*, the color of a component is affected by another one).

For learning a decoupled color representation for each facial component, we present a data augmentation strategy. Specifically, the color image is augmented to different versions with chromatic and spatial transforms, and color representations are extracted from different augmented versions via a shared encoder. By slicing and reorganizing these color representations as a new one, the color representation from each version can be restricted to contribute only to a particular facial component of the colorization result. The su-

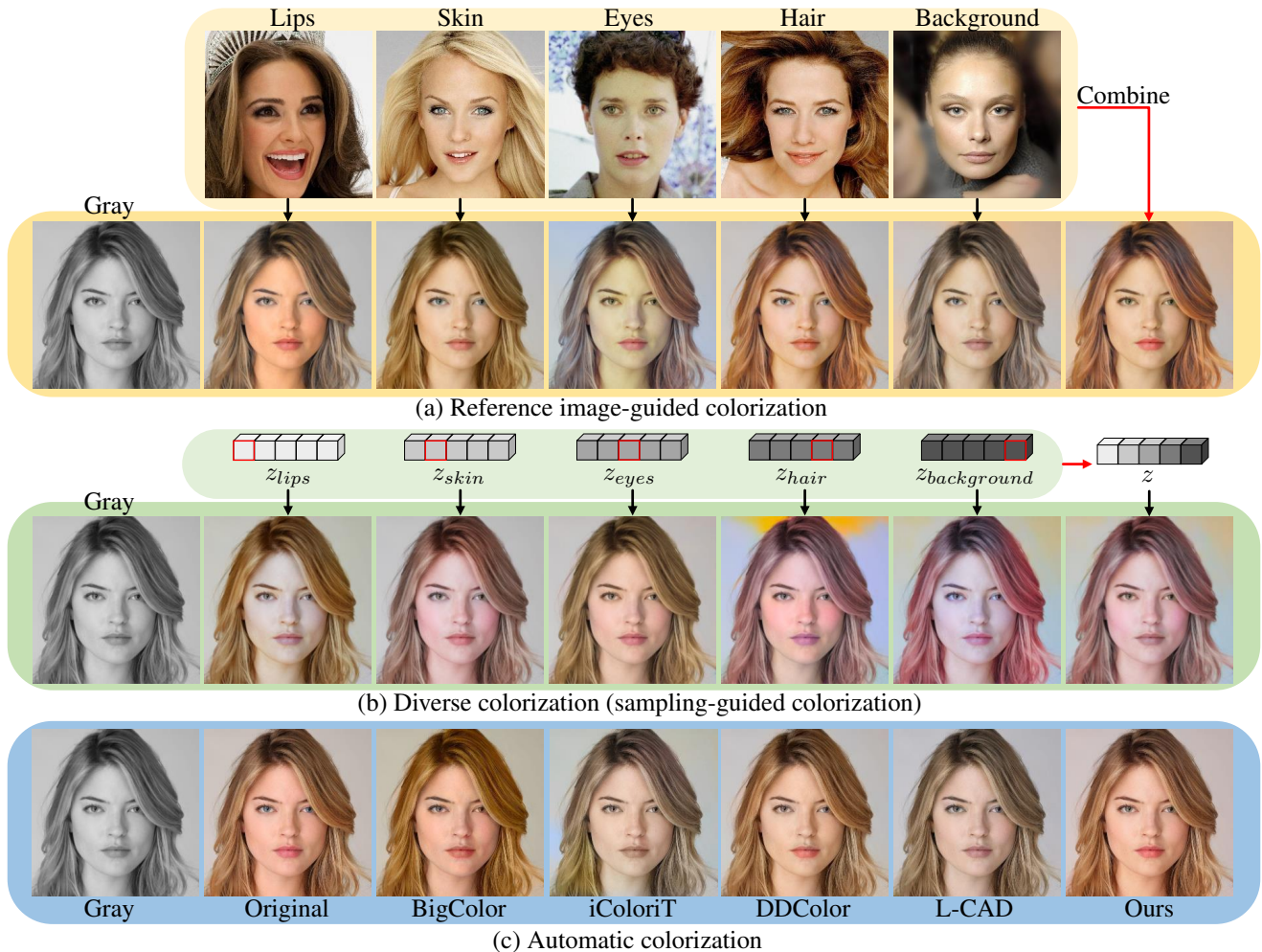


Figure 1: Our method encompasses three colorization approaches, *i.e.*, single- or multi-reference image-guided colorization in (a), sampling-guided colorization in (b), and automatic colorization in (c). In (a), the first row shows five reference images from different identities, while the second row provides the grayscale input, five colorized images referring to the five reference images, and a result whose colorization for different facial components relies on different reference images. In (b), the results are also generated according to the sampled single or multiple color representations. In (c), we give our results under automatic settings and the results of competing methods.

pervision is also a composite color image combined from different augmented versions.

After training, the model can be naturally utilized for reference-based facial image colorization, under both single- and multi-reference settings. Considering that the references are not always easy to prepare, we further expand the application paradigm of the presented FCNet to scenarios with no reference images. For automatic colorization, another encoder is trained to predict the color representation from the input grayscale image (and the face parsing maps). To further introduce randomness and diversity into the prediction results, we also model the color distribution of each facial component via normalizing flow models (Dinh, Krueger, and Bengio 2014; Dinh, Sohl-Dickstein, and Bengio 2016; Kingma and Dhariwal 2018), which can randomly sample

a color representation from the color distribution during the inference stage. The exemplary results of the three colorization approaches are illustrated in Fig. 1.

For evaluating the presented FCNet, comprehensive experiments on facial image colorization are conducted under different settings (*i.e.*, no-, single-, and multi-reference). Both quantitative and qualitative results show the effectiveness of our FCNet. To sum up, the contributions of this paper are as follows.

- Our proposed FCNet decouples the colors of different facial components with the help of facial component priors and a delicately designed data augmentation strategy, enabling individual color control for each facial component and ensuring the controllability of the network.
- Multiple application paradigms, including automatic col-

orization, diverse colorization, and single- and multi-reference-based colorization, are implemented, providing a flexible facial image colorization solution.

- Experiments show that our method not only achieves precise control over the colors of different facial components but also produces colorization results that are more vibrant and diverse than previous approaches.

## Related Work

**Early user-assisted colorization.** Early colorization methods were often user-assisted. One such approach was scribble-based methods, which involved combining segmentation algorithms with manual color assignment by users for each region of the image, resembling a coloring book-like process. Starting from the (Levin, Lischinski, and Weiss 2004), scribble-based colorization was optimized based on spatial continuity using least squares optimization. Subsequent methods (Ironi, Cohen-Or, and Lischinski 2005; Liu et al. 2008) further advanced this technique by introducing improvements and refinements based on the initial framework. Although these approaches can produce visually pleasing results through meticulous user interactions, they often require substantial user efforts. To address this limitation, (Zhang et al. 2017) addressed this limitation by using sparse color points and a neural network for colorization. Other approaches explored using global hints such as color palettes (Bahng et al. 2018; Chang et al. 2015) as constraints instead of dense color points.

**Reference-based methods.** Early approaches in this category transferred the color statistics from a reference image to a grayscale image by utilizing spatial consistency (Chia et al. 2011; Gupta et al. 2012), low-level similarity measures (Liu et al. 2008), or semantic features (Charpiat, Hofmann, and Schölkopf 2008). In recent years, notable advancements have been made by combining deep learning techniques, as demonstrated by prominent works such as (He et al. 2018; Xu et al. 2020; Yoo et al. 2019; Lu et al. 2020; Yin et al. 2021; Ke et al. 2023; Wang et al. 2023). Although this method can achieve visually appealing colorization results and provides control over the image colors, it falls short in precisely specifying the colors of individual objects within each image. Additionally, finding suitable reference images can be challenging.

**Automatic colorization.** Since the advent of (Cheng, Yang, and Sheng 2015), data-driven deep learning methods for colorization have gained significant traction. Notably, (Zhang, Isola, and Efros 2016) introduced the re-balanced multinomial cross-entropy approach to effectively capture the color distribution of individual pixels, while (Deshpande et al. 2017) incorporated a variational autoencoder (VAE) structure to enhance colorization diversity. In recent years, (Su, Chu, and Huang 2020) integrated detection models to leverage detection boxes as informative priors, while (Zhao et al. 2018, 2020) employed segmentation masks as pixel-level priors. Moreover, (Kim et al. 2022; Wu et al. 2021) harnessed pre-trained generative adversarial networks (GANs) to provide valuable color priors, and (Kumar,

Weissenborn, and Kalchbrenner 2021; Ji et al. 2022; Weng et al. 2022; Kang et al. 2023) explored the integration of the Vision Transformer (ViT) (Dosovitskiy et al. 2020) architecture to offer color priors. Recent work (Weng et al. 2024; Liang et al. 2024; Zhang et al. 2023) has proposed a novel automatic colorization methodology leveraging pre-trained diffusion-based models to provide realistic color priors.

## Method

### Overview

In our observation, the main problem with existing image colorization methods on facial images is typically manifested in unnatural and uneven colorization results, which is mainly attributed to the inadequate understanding of facial parts by existing methods. Therefore, the primary objective of this work is to introduce facial component priors into the image colorization procedure. To achieve such an objective, we develop an intuitive solution that simply deploys a face parsing model, which can explicitly provide information about the regions of the facial components. Furthermore, a chromatic and spatial augmentation strategy is presented to force the model to align with the facial component regions. Considering the color consistency of the facial components, we choose to represent the color of each facial component via a low-dimension latent representation, which is then expanded according to the input face structure.

Based on the above analyses, our model is designed with two collaborative modules, *i.e.*, the color representation branch and the colorization network. As shown in Fig. 2, given a grayscale image  $\mathbf{x}^l \in \mathbb{R}^{H \times W \times 1}$ , the color representation branch extracts a color representation from several reference images (each reference image  $\mathbf{x}^{ab} \in \mathbb{R}^{H \times W \times 2}$  has only the ab channels of the CIE-Lab color space). Then, the colorization network can generate the final output given the grayscale input and the color representation. This framework enables each module to focus only on specific problems, avoiding the interference between color prediction and colorization, laying the foundation for expanding the application scenarios of the model. In the following, we will provide more details about the network.

### Color Representation Branch

**Facial Component Priors.** The main purpose of the color representation branch is to indicate the appropriate color for each facial component. Formally speaking, given a reference image  $\mathbf{x}_{ref}$ , we hope that the color representation branch can capture the color of facial components in  $\mathbf{x}_{ref}$ , resulting in a group of color representations  $\mathbf{w}_c$ , where  $c \in \{lips, skin, eyes, hair, background\}$ . In order to equip the model with facial component priors, a face parser  $\mathcal{P}$  is introduced, which provides the masks of the facial components (*i.e.*,  $\mathbf{m}_{ref} = \mathcal{P}(\mathbf{x}_{ref})$ ).

Considering the colorization pipeline, the final result  $\hat{\mathbf{x}} = f(\mathbf{x}^l, g(\mathbf{x}_{ref}, \mathbf{m}_{ref}))$ , where  $f$  and  $g$  denote the colorization network and the color representation branch, respectively. There are no constraints on the decoupling of the color representations for these facial components. In other words, even with the facial component priors (*i.e.*,  $\mathbf{m}_{ref}$ ),

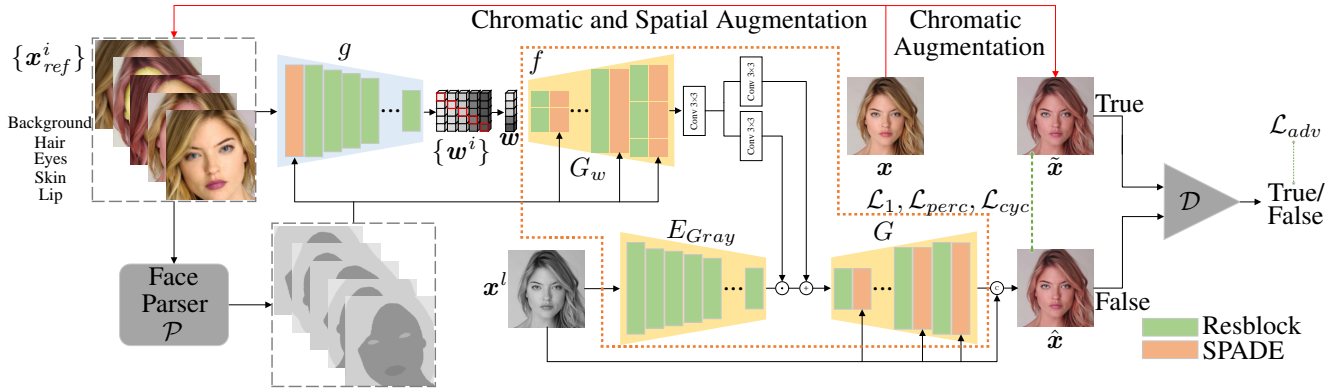


Figure 2: Overview and main training phase of our method. As depicted in the figure, the red arrows represent the data augmentation process. The orange dashed enclosure highlights the colorization network  $f$ .  $\mathcal{D}$  is the discriminator.

the color representations of different facial components are still entangled.

**Data Augmentation.** To learn a decoupled color representation, we present a data augmentation strategy based on existing training data (where only a color image  $x$  and its grayscale version  $x^l$  are available). Specifically, as shown in Fig. 2, the color image  $x$  is augmented from both chromatic and spatial perspectives, resulting in five augmented images  $\{x_{ref}^i\}_{i=0}^4$ , and we take a certain facial component from each  $x_{ref}^i$  to make up a corresponding ground truth  $\tilde{x}$ . In this way, the colorization representation branch can extract a group of colorization representations  $\{w^i\}$  from these augmented images, and each  $w^i$  provide only a certain component in the final  $w$ , i.e.,  $w = [w_{lips}^0, w_{skin}^1, w_{eyes}^2, w_{hair}^3, w_{background}^4]$ .

Without the chromatic augmentation, the spatial augmentation becomes meaningless, where the model can simply rely on a certain reference image. Without the spatial augmentation, the reference images with different postures or those from other identities are unable to be utilized in the inference stage. With both the chromatic and spatial augmentation, the color representation branch can be constrained to obtain the decoupled color representation  $w$ .

### Colorization Network

Given the color representation  $w$ , the colorization network  $f$  can perform the colorization procedure. As shown in Fig. 2,  $f$  consists of two decoders and one encoder. The color representation decoder, denoted as  $G_w$ , processes the color representation  $w$  obtained from the color representation branch, and the resultant feature  $F_w$  serves as a guidance of the colorization. Notably,  $G_w$  employs grouped design (i.e., group convolution) to process the respective parts of  $w$  individually. The gray image encoder, denoted as  $E_{Gray}$ , extracts the feature  $F_l$  from the input grayscale image. The grayscale feature  $F_l$  is modulated by the color representation feature  $F_w$  via an affine transform (i.e., the multiplication and addition operations). Finally, the decoder  $G$  generates the ab channel of the final colorization result  $\hat{x}$ , where

the grayscale input participates in the decoding process and serves as the 1 channel of  $\hat{x}$ . More details about the model can be found in the supplementary materials.

### Learning Objectives

With the color representation branch and the colorization network, the model can be trained simply following existing colorization methods, where  $\ell_1$  loss, perceptual loss (Johnson, Alahi, and Fei-Fei 2016), cycle-consistency loss (Zhu et al. 2017), and adversarial loss (Heusel et al. 2017) are utilized. The only thing worth noting is that, we take all possible data for training, including (1) the original color image  $x$ , (2) each augmented color image  $x_{ref}^i$ , and (3) the composite color image  $\tilde{x}$ . Therefore, the learning objective can be defined by,

$$\mathcal{L} = \mathcal{L}_{adv} + \alpha\mathcal{L}_1 + \beta\mathcal{L}_{perc} + \gamma\mathcal{L}_{cyc}, \quad (1)$$

where  $\alpha$ ,  $\beta$ , and  $\gamma$  are hyper-parameters that are empirically set to 1.0, 0.05, and 1.0, respectively. More details about the loss functions can be found in the supplementary materials.

### Extension to No-reference Scenarios

Given the above network design and learning objectives, the model can be trained for both single- and multi-reference facial image colorization tasks. However, references are not always easy to prepare, which motivates us to extend the model to no-reference scenarios. Thanks to the design of deploying a separate color representation branch, we can safely replace the color representation branch with the alternative modules, which implements the following two application paradigms.

**Automatic Colorization.** Once the FCNet is trained, the color representation  $w$  becomes meaningful. Therefore, as shown in Fig. 3, we can directly learn  $w$  with another encoder  $g_{auto}$ , which predicts a  $w$  from the grayscale input  $x^l$  and the face parsing map  $m^l$ .

**Diverse Colorization.** Given the meaningful  $w$ , we can also learn the distribution of the color representation space



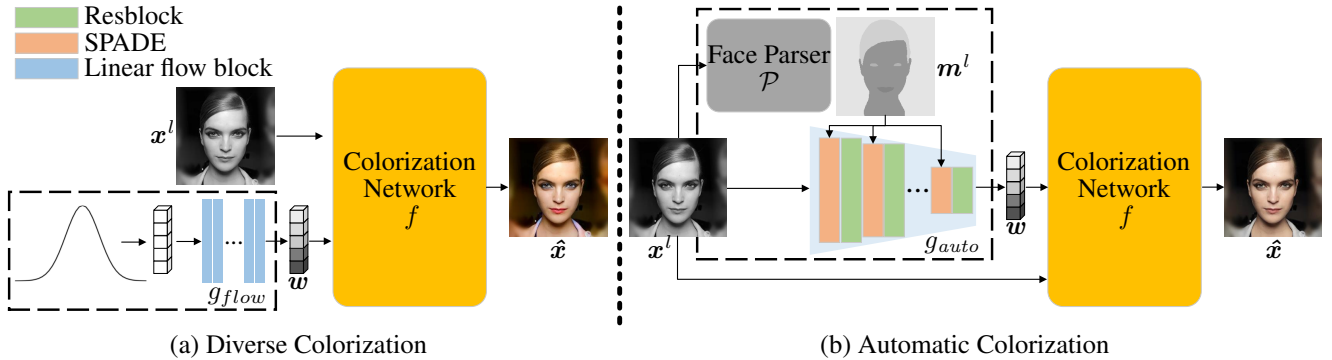


Figure 3: Two application paradigms for No-reference scenarios. (a) denotes the Diverse Colorization, wherein the  $g_{flow}$  can randomly generate a color representation for a given grayscale image  $x^l$  by sampling from a known probability distribution. (b) denotes the Automatic Colorization, wherein the  $g_{auto}$  encodes  $x^l$  and its associated face parsing map  $m^l$  to generate the color representation  $w$ .

with a normalizing flow network  $g_{flow}$ . In this way,  $g_{flow}$  can randomly generate a color representation for a given grayscale input  $x^l$ , which ensures the diversity and randomness. The network structure and learning objective details of  $g_{auto}$  and  $g_{flow}$  can be found in the supplementary materials.

## Experiments

### Experimental Setting

**Datasets.** We conduct our experiments on two aligned facial image datasets. The Flickr-Faces-HQ (FFHQ) dataset (Karras, Laine, and Aila 2019) comprises over 70,000 well-aligned facial images of diverse individuals, which we employ as the training set. Conversely, the CelebA-HQ dataset (Karras et al. 2017) consists of 30,000 high-resolution aligned facial images of celebrity subjects, which we leverage as the test set.

**Evaluation metrics.** Consistent with the previous colorization works, we primarily utilize the Fréchet inception distance (FID) (Heusel et al. 2017) and colorfulness score (CF) as evaluation metrics to assess the effectiveness of our proposed method. For supplementary reference, we also report the Peak Signal-to-Noise Ratio (PSNR) (Huynh-Thu and Ghanbari 2008) and Structural Similarity Measure (SSIM) (Wang et al. 2004) to comprehensively assess the visual perception quality and detailed characteristics of the colorization results.

**Implementation details.** We train our network with the Adam optimizer (Kingma and Ba 2014), and set the hyperparameters  $\beta_1 = 0.5$  and  $\beta_2 = 0.999$ . During the training of our colorization pipeline, we initialize the learning rate to  $5 \times 10^{-5}$  and utilize a batch size of 4. Conversely, when training the subcomponents  $g_{flow}$  and  $g_{auto}$ , we initialize the learning rate to  $1 \times 10^{-3}$  and employ a batch size of 16. Throughout the training process, we resize the training images to dimensions of  $256 \times 256$  pixels and execute the training procedure for a total of 50 epochs over the entirety of the training set. All experiments are conducted on a single

Table 1: Quantitative comparison on CelebA-HQ dataset. The method ranked first for each metric is displayed in bold, and the method ranked second is underlined.

| Methods          | FID↓        | CF↑          | PSNR↑        | SSIM↑         |
|------------------|-------------|--------------|--------------|---------------|
| Colorful (2016)  | 11.41       | 37.82        | 24.69        | 0.9419        |
| InstColor (2020) | 8.99        | 37.02        | 25.46        | <u>0.9940</u> |
| GCP (2021)       | 10.29       | 33.70        | 24.33        | 0.9937        |
| Unicolor (2022)  | 6.17        | 37.41        | 23.21        | 0.9406        |
| DisColor (2022)  | 8.79        | 43.37        | 23.72        | 0.9934        |
| CT2 (2022)       | 8.61        | 43.33        | 24.55        | 0.9415        |
| BigColor (2022)  | 6.34        | 42.99        | 23.34        | 0.9339        |
| iColoriT (2023)  | 12.68       | 32.32        | <u>27.53</u> | 0.9809        |
| DDColor (2023)   | <u>3.80</u> | <b>49.71</b> | 24.25        | 0.9936        |
| L-CAD (2024)     | 7.43        | 28.73        | 23.86        | 0.9911        |
| Ours             | <b>3.60</b> | <u>43.73</u> | <b>30.50</b> | <b>0.9946</b> |

NVIDIA RTX A6000 GPU. For detailed information regarding the experimental hardware and software environment, as well as the implementation details, please refer to the supplementary materials.

### Comparison with Previous Methods

**Quantitative comparison.** We evaluate the performance of the automatic colorization results of our proposed method against prior techniques on the test dataset, reporting quantitative results across four distinct metrics in Tab. 1. The proposed method is evaluated against a selection of the most recent and representative colorization techniques, including Colorful (Zhang, Isola, and Efros 2016), InstColor (Su, Chu, and Huang 2020), GCP (Wu et al. 2021), Unicolor (Huang, Zhao, and Liao 2022), DisColor (Xia et al. 2022), CT2 (Weng et al. 2022), BigColor (Kim et al. 2022), iColoriT (Yun et al. 2023), DDColor (Kang et al. 2023), and L-CAD (Weng et al. 2024). Experimental evaluations utilize the official codebases and pre-trained model weights provided by the respective authors, as well as the automatic col-

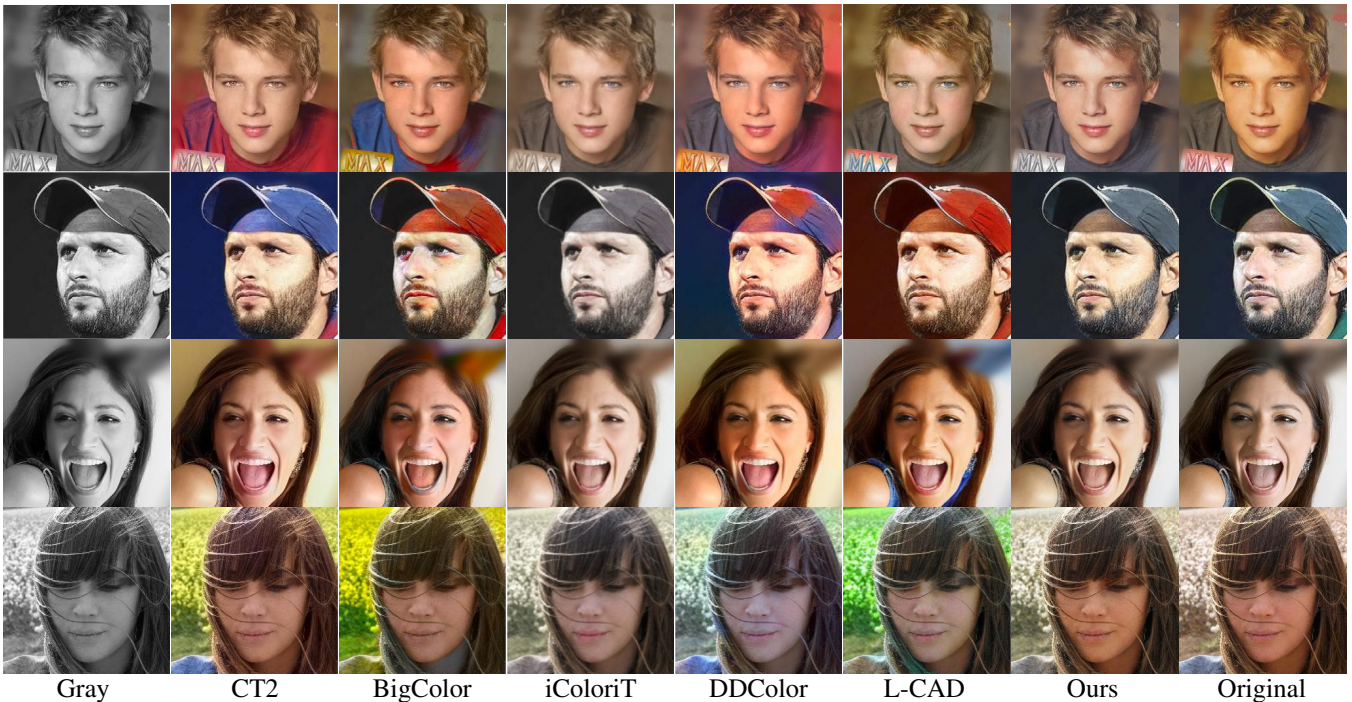


Figure 4: The qualitative results of our method and automatic colorization baseline methods.

orization approaches described in their papers. The proposed method achieves the lowest FID, indicating superior colorization quality and fidelity. In terms of colorfulness score, which reflects color richness, the approach ranks second among the evaluated techniques. However, excessive colorfulness does not necessarily equate to optimal visual quality. Our proposed method exhibits the best performance on the PSNR and SSIM pixel-wise evaluation metrics, demonstrating the high quality of the generated images.

**Qualitative evaluation.** Fig. 4 showcases representative automatic colorization results from our baseline methods. Note that the original colored images serve as reference benchmarks rather than definitive standards. Our results demonstrate the minimal degree of color bleeding and the most naturalistic visual appearance. Furthermore, our colorization outputs do not present an excessive variety of colors that would lead to an unrealistic appearance. Fig. 5 presents qualitative comparisons between the proposed method’s reference image-guided colorization results and those of the latest representative reference image-guided colorization techniques, including WCT2 (Yoo et al. 2019), Gray2ColorNet (Lu et al. 2020), TFcolor (Yin et al. 2021), Uicolor (Huang, Zhao, and Liao 2022), and PDNLA-Net (Wang et al. 2023). Early techniques like WCT2 (Yoo et al. 2019) fail to consider the input image’s grayscale values. Global color transfer methods, exemplified by Gray2ColorNet (Lu et al. 2020), exhibit difficulty accurately specifying individual component hues. Uicolor (Huang, Zhao, and Liao 2022) and PDNLA-Net (Wang et al. 2023) concomitantly exhibit an inability to accurately specify intricate details, such as iris hue, culminating in un-

desirable color bleeding. Furthermore, to demonstrate the visual effects of our method under various color control approaches, we have introduced more reference image-guided colorization results guided by referencing single or multiple image(s) and diverse colorization results guided by single or multiple sampling(s) from Gaussian distribution. These additional results are included in the supplementary material.

### Ablation Study

We conducted ablation studies to assess the impact of several important designs in our model and training. The quantitative results were obtained on the full test set. Unless explicitly stated, we maintained a consistent training configuration during ablation studies.

**Color representation branch.** The proposed color representation branch  $g$  decouples the color information from the facial components to obtain the color representation  $w$ .

Following the removal of the color representation decoder  $G_w$  structure associated with the  $g$ , the remaining  $E_{Gray}$  and  $G$  serve as the baseline for the subsequent ablation study. As evidenced in Tab. 2, the quantitative results of the automatic colorization approach underscore the crucial role of the color representation branch in enhancing the various quantitative performance metrics. Please refer to the supplementary materials for the qualitative results.

**Data Augmentation.** During the training phase, to obtain a more effectively decoupled color representation, we employed chromatic augmentation techniques such as color jittering, as well as spatial augmentation approaches including affine transformations and flipping. We conduct ablation





Figure 5: The qualitative results of our method and reference image-based colorization baseline methods.

Table 2: Quantitative comparison on Ablation studies. The method ranked first for each metric is displayed in bold, and the method ranked second is underlined.

| Models               | Color Representation Branch | Data Augmentation      |                      | Grouped design | FID↓        | CF↑          | PSNR↑        | SSIM↑         |
|----------------------|-----------------------------|------------------------|----------------------|----------------|-------------|--------------|--------------|---------------|
|                      |                             | Chromatic Augmentation | Spatial Augmentation |                |             |              |              |               |
| Baseline             |                             |                        |                      |                | 10.43       | 43.07        | 24.53        | 0.9937        |
| w/o Data Augmentaion | ✓                           |                        |                      | ✓              | 7.84        | 42.51        | 25.89        | 0.9942        |
|                      | ✓                           | ✓                      |                      | ✓              | 7.32        | <b>43.92</b> | <u>28.01</u> | <u>0.9945</u> |
|                      | ✓                           |                        | ✓                    | ✓              | 5.45        | 43.35        | 26.91        | <b>0.9946</b> |
| w/o Grouped design   | ✓                           | ✓                      | ✓                    |                | <u>5.38</u> | 43.29        | 26.77        | <b>0.9946</b> |
| Ours                 | ✓                           | ✓                      | ✓                    | ✓              | <b>3.60</b> | <u>43.73</u> | <b>30.50</b> | <b>0.9946</b> |

studies to demonstrate the necessity of these two types of augmentation and to elucidate their respective contributions. Tab. 2 demonstrates that chromatic augmentation enhanced the CF metric, indicating its capacity to expand the network’s color coverage range. Conversely, spatial augmentation reduced the FID metric, showcasing its ability to improve the fidelity of the generated images. Employing both augmentation approaches simultaneously optimized these two metrics, establishing a favorable trade-off. Please refer to the supplementary materials for the qualitative results.

**Grouped design.** The  $G_w$  module is designed with a grouped structure to process the individual parts of  $w$  separately. To evaluate the contribution of this design, we conducted comparative experiments, as detailed in Tab. 2. We performed comparative experiments to assess the impact of this architectural design on the network’s controllability, as detailed in Tab. 2. The results demonstrate that omitting the grouped design leads to deficiencies across various quantita-

tive metrics, compared to our intact approach. Furthermore, the qualitative analysis presented in the supplementary materials reveals that irrespective of the coloring method, removing the grouped structure results in color bleeding and spills onto other regions of the face.

## Conclusion

In this work, we have developed a novel framework for component-specific facial colorization that offers advanced control and versatility. The core innovation of our approach lies in the decoupling of facial component colors into a dedicated color representation within our color representation branch. This design choice enables the independent specification of colors for each facial component, thereby facilitating diverse color control.

## References

- Bahng, H.; Yoo, S.; Cho, W.; Park, D. K.; Wu, Z.; Ma, X.; and Choo, J. 2018. Coloring with words: Guiding image colorization through text-based palette generation. In *Proceedings of the european conference on computer vision (eccv)*, 431–447.
- Chang, H.; Fried, O.; Liu, Y.; DiVerdi, S.; and Finkelstein, A. 2015. Palette-based photo recoloring. *ACM Trans. Graph.*, 34(4): 139–1.
- Charpiat, G.; Hofmann, M.; and Schölkopf, B. 2008. Automatic image colorization via multimodal predictions. In *Computer Vision—ECCV 2008: 10th European Conference on Computer Vision, Marseille, France, October 12–18, 2008, Proceedings, Part III 10*, 126–139. Springer.
- Cheng, Z.; Yang, Q.; and Sheng, B. 2015. Deep colorization. In *Proceedings of the IEEE international conference on computer vision*, 415–423.
- Chia, A. Y.-S.; Zhuo, S.; Gupta, R. K.; Tai, Y.-W.; Cho, S.-Y.; Tan, P.; and Lin, S. 2011. Semantic colorization with internet images. *ACM Transactions on Graphics (ToG)*, 30(6): 1–8.
- Deshpande, A.; Lu, J.; Yeh, M.-C.; Jin Chong, M.; and Forsyth, D. 2017. Learning diverse image colorization. In *Proceedings of the IEEE conference on computer vision and pattern recognition*, 6837–6845.
- Dinh, L.; Krueger, D.; and Bengio, Y. 2014. Nice: Non-linear independent components estimation. *arXiv preprint arXiv:1410.8516*.
- Dinh, L.; Sohl-Dickstein, J.; and Bengio, S. 2016. Density estimation using real nvp. *arXiv preprint arXiv:1605.08803*.
- Dosovitskiy, A.; Beyer, L.; Kolesnikov, A.; Weissenborn, D.; Zhai, X.; Unterthiner, T.; Dehghani, M.; Minderer, M.; Heigold, G.; Gelly, S.; et al. 2020. An image is worth 16x16 words: Transformers for image recognition at scale. *arXiv preprint arXiv:2010.11929*.
- Gupta, R. K.; Chia, A. Y.-S.; Rajan, D.; Ng, E. S.; and Zhiyong, H. 2012. Image colorization using similar images. In *Proceedings of the 20th ACM international conference on Multimedia*, 369–378.
- He, M.; Chen, D.; Liao, J.; Sander, P. V.; and Yuan, L. 2018. Deep exemplar-based colorization. *ACM Transactions on Graphics (TOG)*, 37(4): 1–16.
- Heusel, M.; Ramsauer, H.; Unterthiner, T.; Nessler, B.; and Hochreiter, S. 2017. Gans trained by a two time-scale update rule converge to a local nash equilibrium. *Advances in neural information processing systems*, 30.
- Huang, Z.; Zhao, N.; and Liao, J. 2022. UniColor: A Unified Framework for Multi-Modal Colorization with Transformer. *ACM Trans. Graph.*, 41(6).
- Huynh-Thu, Q.; and Ghanbari, M. 2008. Scope of validity of PSNR in image/video quality assessment. *Electronics letters*, 44(13): 800–801.
- Iizuka, S.; and Simo-Serra, E. 2019. Deepremaster: temporal source-reference attention networks for comprehensive video enhancement. *ACM Transactions on Graphics (TOG)*, 38(6): 1–13.
- Ironi, R.; Cohen-Or, D.; and Lischinski, D. 2005. Colorization by Example. *Rendering techniques*, 29: 201–210.
- Ji, X.; Jiang, B.; Luo, D.; Tao, G.; Chu, W.; Xie, Z.; Wang, C.; and Tai, Y. 2022. ColorFormer: Image colorization via color memory assisted hybrid-attention transformer. In *European Conference on Computer Vision*, 20–36. Springer.
- Johnson, J.; Alahi, A.; and Fei-Fei, L. 2016. Perceptual losses for real-time style transfer and super-resolution. In *Computer Vision—ECCV 2016: 14th European Conference, Amsterdam, The Netherlands, October 11–14, 2016, Proceedings, Part II 14*, 694–711. Springer.
- Kang, X.; Yang, T.; Ouyang, W.; Ren, P.; Li, L.; and Xie, X. 2023. Ddcolor: Towards photo-realistic image colorization via dual decoders. In *Proceedings of the IEEE/CVF International Conference on Computer Vision*, 328–338.
- Karras, T.; Aila, T.; Laine, S.; and Lehtinen, J. 2017. Progressive growing of gans for improved quality, stability, and variation. *arXiv preprint arXiv:1710.10196*.
- Karras, T.; Laine, S.; and Aila, T. 2019. A style-based generator architecture for generative adversarial networks. In *Proceedings of the IEEE/CVF conference on computer vision and pattern recognition*, 4401–4410.
- Ke, Z.; Liu, Y.; Zhu, L.; Zhao, N.; and Lau, R. W. 2023. Neural preset for color style transfer. In *Proceedings of the IEEE/CVF Conference on Computer Vision and Pattern Recognition*, 14173–14182.
- Kim, G.; Kang, K.; Kim, S.; Lee, H.; Kim, S.; Kim, J.; Baek, S.-H.; and Cho, S. 2022. BigColor: Colorization using a generative color prior for natural images. In *European Conference on Computer Vision*, 350–366. Springer.
- Kingma, D. P.; and Ba, J. 2014. Adam: A method for stochastic optimization. *arXiv preprint arXiv:1412.6980*.
- Kingma, D. P.; and Dhariwal, P. 2018. Glow: Generative flow with invertible 1x1 convolutions. *Advances in neural information processing systems*, 31.
- Kumar, M.; Weissenborn, D.; and Kalchbrenner, N. 2021. Colorization transformer. *arXiv preprint arXiv:2102.04432*.
- Levin, A.; Lischinski, D.; and Weiss, Y. 2004. Colorization using optimization. In *ACM SIGGRAPH 2004 Papers*, 689–694.
- Liang, Z.; Li, Z.; Zhou, S.; Li, C.; and Loy, C. C. 2024. Control Color: Multimodal Diffusion-based Interactive Image Colorization. *arXiv preprint arXiv:2402.10855*.
- Liu, X.; Wan, L.; Qu, Y.; Wong, T.-T.; Lin, S.; Leung, C.-S.; and Heng, P.-A. 2008. Intrinsic colorization. In *ACM SIGGRAPH Asia 2008 papers*, 1–9.
- Lu, P.; Yu, J.; Peng, X.; Zhao, Z.; and Wang, X. 2020. Gray2colornet: Transfer more colors from reference image. In *Proceedings of the 28th ACM international conference on multimedia*, 3210–3218.
- Qu, Y.; Wong, T.-T.; and Heng, P.-A. 2006. Manga colorization. *ACM Transactions on Graphics (ToG)*, 25(3): 1214–1220.
- Su, J.-W.; Chu, H.-K.; and Huang, J.-B. 2020. Instance-aware image colorization. In *Proceedings of the IEEE/CVF*



- Conference on Computer Vision and Pattern Recognition*, 7968–7977.
- Tsaftaris, S. A.; Casadio, F.; Andral, J.-L.; and Katsaggelos, A. K. 2014. A novel visualization tool for art history and conservation: Automated colorization of black and white archival photographs of works of art. *Studies in conservation*, 59(3): 125–135.
- Vitoria, P.; Raad, L.; and Ballester, C. 2020. Chromagan: Adversarial picture colorization with semantic class distribution. In *Proceedings of the IEEE/CVF winter conference on applications of computer vision*, 2445–2454.
- Wang, H.; Zhai, D.; Liu, X.; Jiang, J.; and Gao, W. 2023. Unsupervised deep exemplar colorization via pyramid dual non-local attention. *IEEE Transactions on Image Processing*.
- Wang, Z.; Bovik, A. C.; Sheikh, H. R.; and Simoncelli, E. P. 2004. Image quality assessment: from error visibility to structural similarity. *IEEE transactions on image processing*, 13(4): 600–612.
- Weng, S.; Sun, J.; Li, Y.; Li, S.; and Shi, B. 2022. CT 2: Colorization transformer via color tokens. In *European Conference on Computer Vision*, 1–16. Springer.
- Weng, S.; Zhang, P.; Li, Y.; Li, S.; Shi, B.; et al. 2024. L-cad: Language-based colorization with any-level descriptions using diffusion priors. *Advances in Neural Information Processing Systems*, 36.
- Wu, Y.; Wang, X.; Li, Y.; Zhang, H.; Zhao, X.; and Shan, Y. 2021. Towards vivid and diverse image colorization with generative color prior. In *Proceedings of the IEEE/CVF international conference on computer vision*, 14377–14386.
- Xia, M.; Hu, W.; Wong, T.-T.; and Wang, J. 2022. Disentangled image colorization via global anchors. *ACM Transactions on Graphics (TOG)*, 41(6): 1–13.
- Xu, Z.; Wang, T.; Fang, F.; Sheng, Y.; and Zhang, G. 2020. Stylization-based architecture for fast deep exemplar colorization. In *Proceedings of the IEEE/CVF Conference on Computer Vision and Pattern Recognition*, 9363–9372.
- Yin, W.; Lu, P.; Zhao, Z.; and Peng, X. 2021. “Yes,” Attention Is All You Need”, for Exemplar based Colorization. In *Proceedings of the 29th ACM international conference on multimedia*, 2243–2251.
- Yoo, J.; Uh, Y.; Chun, S.; Kang, B.; and Ha, J.-W. 2019. Photorealistic style transfer via wavelet transforms. In *Proceedings of the IEEE/CVF international conference on computer vision*, 9036–9045.
- Yun, J.; Lee, S.; Park, M.; and Choo, J. 2023. iColoriT: Towards propagating local hints to the right region in interactive colorization by leveraging vision transformer. In *Proceedings of the IEEE/CVF Winter Conference on Applications of Computer Vision*, 1787–1796.
- Zhang, R.; Isola, P.; and Efros, A. A. 2016. Colorful image colorization. In *Computer Vision—ECCV 2016: 14th European Conference, Amsterdam, The Netherlands, October 11–14, 2016, Proceedings, Part III 14*, 649–666. Springer.
- Zhang, R.; Zhu, J.-Y.; Isola, P.; Geng, X.; Lin, A. S.; Yu, T.; and Efros, A. A. 2017. Real-time user-guided image colorization with learned deep priors. *arXiv preprint arXiv:1705.02999*.
- Zhang, Y.; Wei, Y.; Jiang, D.; Zhang, X.; Zuo, W.; and Tian, Q. 2023. Controlvideo: Training-free controllable text-to-video generation. *arXiv preprint arXiv:2305.13077*.
- Zhao, J.; Han, J.; Shao, L.; and Snoek, C. G. 2020. Pixelated semantic colorization. *International Journal of Computer Vision*, 128: 818–834.
- Zhao, J.; Liu, L.; Snoek, C. G.; Han, J.; and Shao, L. 2018. Pixel-level semantics guided image colorization. *arXiv preprint arXiv:1808.01597*.
- Zhu, J.-Y.; Park, T.; Isola, P.; and Efros, A. A. 2017. Unpaired image-to-image translation using cycle-consistent adversarial networks. In *Proceedings of the IEEE international conference on computer vision*, 2223–2232.